SCIENCE CHINA
Physics, Mechanics & Astronomy

• Article •

April 2018 Vol. 61 No. 4: 040311
https://doi.org/10.1007/s11433-017-9101-4

Spontaneous decoherence of coupled harmonic oscillators confined in a ring

ZhiRui Gong[1,2*], ZhenWei Zhang[1], DaZhi Xu[2,3], Nan Zhao[2], and ChangPu Sun[2]

[1] *College of Physics and Energy, Shenzhen University, Shenzhen 518060, China;*
[2] *Beijing Computational Science Research Center, Beijing 100084, China;*
[3] *Center for Quantum Technology Research, School of Physics, Beijing Institute of Technology, Beijing 100081, China*

Received July 18, 2017; accepted August 31, 2017; published online January 22, 2018

We study the spontaneous decoherence of coupled harmonic oscillators confined in a ring container, where the nearest-neighbor harmonic potentials are taken into consideration. Without any external symmetry-breaking field or surrounding environment, the quantum superposition state prepared in the relative degrees of freedom gradually loses its quantum coherence spontaneously. This spontaneous decoherence is interpreted by the gauge couplings between the center-of-mass and the relative degrees of freedoms, which actually originate from the symmetries of the ring geometry and the corresponding nontrivial boundary conditions. In particular, such spontaneous decoherence does not occur at all at the thermodynamic limit because the nontrivial boundary conditions become the trivial Born-von Karman boundary conditions when the perimeter of the ring container tends to infinity. Our investigation shows that a thermal macroscopic object with certain symmetries has a chance for its quantum properties to degrade even without applying an external symmetry-breaking field or surrounding environment.

spontaneous quantum decoherence, periodic boundary condition, gauge interaction

PACS number(s): 03.65.Yz, 05.30.Jp, 03.65. C w, 03.75.Kk

Citation: Z. R. Gong, Z. W. Zhang, D. Z. Xu, N. Zhao, and C. P. Sun, Spontaneous decoherence of coupled harmonic oscillators confined in a ring, Sci. China-Phys. Mech. Astron. **61**, 040311 (2018), https://doi.org/10.1007/s11433-017-9101-4

1 Introduction

Quantum decoherence has been a subject of active research since quantum mechanics was established [1]. The revival of the study of decoherence as a popular subject originates from the development of quantum information. As the physical states in quantum mechanics are described by the superposition of some eigenstates, the coherence existing between different eigenstates is an important criteria for whether the quantum properties of the system remain. In this sense, quantum decoherence explains the emergence of the classical limit in a quantum system, which apparently determines the quantum-classical boundary [2-5], and plays a crucial role in quantum information technologies such as quantum state transfers [6-8], quantum error corrections [9], and so on.

Originally, quantum decoherence was the name for the collapse of the wave function in the Copenhagen interpretation [10]. Instead of generating actual wave function collapse, it only gives the appearance of wave function collapse. Nowadays, studies on decoherence focus on the quantum correlation between a system and its environment [11-14]. As commonly understood, the decoherence process can be viewed as the quantum system losing information to its environment. Mathematically, losing information in the decoherence process can be defined as the disappearance of the off-diagonal elements of the system's reduced density matrix.

*Corresponding author (email: gongzr@szu.edu.cn)

© Science China Press and Springer-Verlag GmbH Germany 2018

A perfect decoherence process requires that the environment approaches its thermodynamic limit, whose infinite degrees of freedom guarantees the infinitely long recurrence time of the decoherence process [15-21].

To reveal the mechanism of quantum decoherence, Heisenberg introduced a random phase factor according to the uncertainty principle. This phase factor also results in the randomness of the coefficients of the off-diagonal elements in the system's reduced density matrix, whose average over time tends to zero. However, the uncertainty principle is not the only mechanism to cause decoherence, which has been verified experimentally [22, 23]. Additionally, in some specific systems, such as quantum non-demolition measurement, the Heisenberg uncertainty does not cause the randomness of the phase factor due to the relationship between the measured variables and the Hamiltonian of the system. In general, the random factor originates from the interaction between the quantum system and its environment. In contrast to the external environment mentioned above, we are more interested in an internal one [24, 25]. For most quantum systems, only some subspaces of the system's complete Hilbert space are concentrated on, whose adjoint space can be regarded as the "internal" environment with interactions between these two spaces, such as the spin-orbit interaction, electron-phonon interaction, and so on. Instead of the infinite degrees of freedom the external environment has, the internal environment only possesses a few degrees of freedom.

In contrast with the usual decoherence, which always involves the interaction between the system and the environment, decoherence can also result from the symmetries or non-trivial boundary conditions of the system plus the environment. Since there is no obvious interaction between the system and environment in the latter case, such decoherence is called "spontaneous decoherence." Previous theoretical research has indicated that, due to the spontaneous symmetry breaking [26-29] in association with quantum phase transitions [30], quantum decoherence emerges in a multiparticle system when a small but finite symmetry breaking field is added to a closed symmetric quantum system. When the symmetry is broken, a series of thin spectra emerge in the vicinity of the original energy levels. The subtle energy differences of the thin spectra actually result in spontaneous decoherence. Recently, researchers have shown that spontaneous decoherence can also be induced by gravitational time dilation [31-33].

In this paper, we shall study the spontaneous decoherence of a closed multiparticle system without symmetry breaking. Considering N coupled harmonic oscillators confined in a ring container, the Hamiltonian can be decoupled into the center-of-mass motion and $N-1$ relative motions. It is essential that the harmonic potentials between oscillators are periodic because of the ring configuration. Such a bosonic multiparticle system possesses $U(1)\otimes C_N$ symmetry, where the continuous $U(1)$-symmetry and discrete C_N-symmetry respectively relate the center-of-mass and relative motions' symmetries. Then, nontrivial boundary conditions emerge in order to guarantee the single-valuedness of the wave function, which eventually results in the total energy spectrum not only depending on the excitations of the relative motions, but also on the total momentum corresponding to the center-of-mass motion. Similar to the Aharonov-Bohm effect, the nontrivial boundary conditions are actually equivalent to applying an induced gauge field [34]. This gauge coupling between the center-of-mass motion and relative motions introduces a series of thin spectra of the total momentum, which contributes to the decoherence process of the relative motions. If the center-of-mass motion is not condensed to the state with a single momentum, the spontaneous decoherence process occurs in the superposition states of the relative motions. Since there is no environment or symmetry-breaking field at all, the decoherence in our model is definitely intrinsic and its dynamical process is spontaneous. The paradox of such spontaneous decoherence is that the information represented by the quantum coherence is mysteriously missing in a completely closed system. The key point to explaining this is that the center-of-mass motion actually acts like a surrounding environment to the relative motions we concentrated on. The information is only transferred from the subspace of the complete Hilbert space into its adjoint space.

This article is arranged as follows. We describe the multiparticle model and derive the nontrivial boundary conditions in sect. 2. Then, the explicit total energy spectrum including all the thin spectra is obtained in sect. 3. In sect. 4, we demonstrate how the thin spectra contribute to the dynamic decoherence process. We conclude in sect. 5.

2 Coupled harmonic oscillators confined in a ring container

2.1 Model setup

To investigate the mechanism of decoherence due to the symmetries of system, we consider a bosonic multiparticle system confined in a ring container (Figure 1(a)), which is modeled as N coupled harmonic oscillators with the Hamiltonian

$$\hat{H}=\sum_{j=1}^{N}\left[\frac{\hat{p}_j^2}{2m}+V(\hat{x}_j-\hat{x}_{j+1})\right], \tag{1}$$

where

$$V(\hat{x}_j-\hat{x}_{j+1})=\frac{\kappa}{2}\left(\hat{x}_j-\hat{x}_{j+1}\right)^2 \tag{2}$$

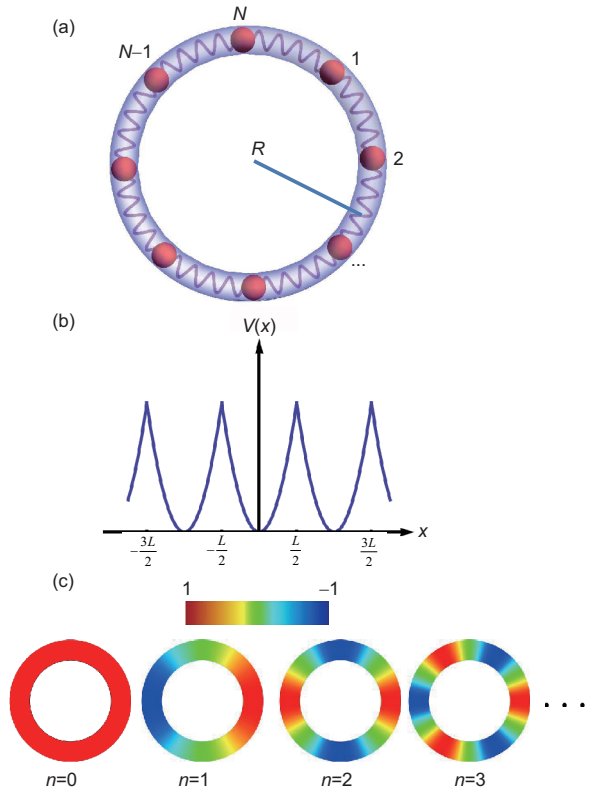

Figure 1 (Color online) (a) Schematic illustration of the coupled harmonic oscillators confined in a ring container. Here, the light blue torus and the red spheres represent the ring container with radius R and the oscillators, respectively; (b) schematic illustration of the periodic harmonic potential. Here, x denotes any displacement difference between the nearest-neighbor oscillators; (c) schematic illustration of the real part of the center-of-mass motion wavefunction versus the displacement X_0 for the first four values of the quantum number n.

are the harmonic potentials between nearest-neighbor oscillators. Here, $\hat{p}_j$ and $\hat{x}_j$ are the momentum and the displacement of the j-th oscillator. For the sake of simplicity, the oscillator mass m and the spring constant κ are identical for all oscillators, and the system is considered to be one-dimensional since the cross section radius of the ring container is much smaller than the radius of the ring R. Our model is analogous to the textbook example of phonons in solid state physics with the Born-von Karman boundary condition. However, there is an essential difference between these two models. Since the harmonic oscillator potentials for the phonons are effective ones, which result from the Coulomb interaction between the electrons and the nuclei, the Hamiltonian would not be changed if the positions of any two particles are switched. However, in our model, the harmonic oscillator potentials are inherent and the Hamiltonian would be changed if the positions of any two particles are switched. In the present situation, the oscillators can potentially move far away from their equilibrium positions if their kinetic energies are sufficiently large. In this case, the harmonic potentials become periodic as:

$$V(x_j - x_{j+1} + nL) = V(x_j - x_{j+1}), \tag{3}$$

when any of the displacement differences between the nearest-neighbor oscillators are augmented by nL (n is an integer). This periodic potential is schematically plotted in Figure 1(b). Here, $L = 2\pi R$ is the perimeter of the ring container. Since the harmonic potentials only involve the displacement differences between the nearest-neighbor oscillators, the above coupled-oscillator system can be decoupled into N oscillators, which correspond to the center-of-mass motion and $(N-1)$ relative motions.

To decouple the system into N oscillators, we successively perform the Fourier transformation $\left(\hat{q}_j = \hat{p}_j, \hat{x}_j\right)$:

$$\hat{Q}_k = \begin{cases} \sqrt{\frac{2}{N}} \sum_{j=1}^{N} \hat{q}_j \cos\left(\frac{2\pi kj}{N}\right), & 1 \le k \le \frac{N}{2}, \\ \sqrt{\frac{2}{N}} \sum_{j=1}^{N} \hat{q}_j \sin\left(\frac{2\pi kj}{N}\right), & k > \frac{N}{2}, \end{cases} \tag{4}$$

where $\hat{Q}_k = \hat{P}_k, \hat{X}_k$ $(k = 1, \cdots, N-1)$ are the momenta and the displacements of the $N-1$ independent relative motions. Besides the relative motions, there is a unique center-of-mass motion, whose momentum and displacement are described as $\hat{P}_0 = \sum_{j=1}^{N} \hat{p}_j$ and $\hat{X}_0 = 1/N \sum_{j=1}^{N} \hat{x}_j$, respectively. We introduce the different forms for the momenta and the displacements when $1 \le k \le N/2$ and $k > N/2$. After the Fourier transformation, the Hamiltonian becomes N decoupled harmonic oscillators:

$$\hat{H} = \hat{H}_0 + \sum_{k=1}^{N-1} \hat{H}_k, \tag{5a}$$

$$\hat{H}_k = \frac{\hat{P}_k^2}{2m} + \frac{\kappa}{2}\left(2\sin\frac{\pi k}{N}\right)^2 \hat{X}_k^2. \tag{5b}$$

It is noticeable that the zeroth Hamiltonian

$$\hat{H}_0 = \frac{\hat{P}_0^2}{4mN} = \frac{1}{2mN}\left(\sum_{j=1}^{N} \hat{p}_j\right)^2 \tag{6}$$

describes the center-of-mass motion of the multiple particle system, which is regarded as a whole as carrying a kinetic energy associated with the total mass of the system. The rest part of the Hamiltonian $\hat{H}_R = \hat{H} - \hat{H}_0 = \sum_{k=1}^{N-1} \hat{H}_k$, describes the decoupled $N-1$ relative motions. It should be noted that the Hamiltonian can be completely separated into the center-of-mass motion part and the relative motions part only when the adjacent particles couple to each other with harmonic oscillator potentials, as shown in eq. (2). Obviously, each relative mode is described by a periodic harmonic oscillator. Although the periodicities of these relative motions are no longer simply demonstrated, the sum of all the relative harmonic oscillators potentials still possesses the periodicities

shown in eq. (3). By solving the eigenvalue problem for the system, we can obtain the thin spectrum that plays an essential role in our spontaneous quantum decoherence process.

It should be emphasized that although in a ring geometry the displacement operator is no longer a physical observable [35, 36] that needs to be replaced by $\exp(\mathrm{i}\theta)$, with $\theta = \hat{x}/R$, the momentum operator is still a physical observable due to the translational symmetry. Under this circumstance, the commutation relation between the displacement and the momentum becomes $\left[M_j, \exp(\alpha \mathrm{i}\theta_k)\right] = \alpha\delta_{j,k}\exp(\alpha \mathrm{i}\theta_k)$ with the corresponding angle and angular momentum operators $\theta_k = \frac{x_k}{R}$ and $M_j = \frac{R}{\hbar}p_j$, respectively. It is easy to prove that the Fourier transformation we applied in eq. (4) guarantees that the transformed displacements and momentum still follow the same commutation relation. In this sense, the center-of-mass motion and relative motions are completely independent.

2.2 Origin of the thin spectrum

Although the center-of-mass motion and relative motions seem independent of each other in the Hamiltonian, there is a gauge coupling between them due to the symmetry of the system. For a given quantum system, the energy spectrum and eigen-states are not only governed by its Hamiltonian, but also by the boundary conditions, which depend on the symmetries of the system [34]. We will find the boundary conditions for our system as follows.

We first analyze the existing symmetries of the system shown in Figure 1(a). If all the oscillator displacements x_j ($j = 1, \ldots, N$) are augmented by the same increment δx, the Hamiltonian remains unchanged, which means the system possesses $U(1)$-symmetry. Since the Hamiltonian has been decoupled as eq. (5a), the eigenstate of the system is obtained as:

$$\Psi(\boldsymbol{X}) = \exp\left(\frac{\mathrm{i}}{\hbar}P_0 X_0\right)\chi(\boldsymbol{X}), \tag{7}$$

where the plane wave $\exp(\mathrm{i}P_0X_0/\hbar)$ and the product state

$$\chi(\boldsymbol{X}) = \prod_{j=1}^{N-1}\chi_j\left(X_j\right) \tag{8}$$

describe the center-of-mass motion and the relative motions, respectively. Here, the vector $\boldsymbol{X} = \{X_1, X_2, \ldots, X_{N-1}\}$ represents the displacements of the relative motions, and $\boldsymbol{x} = \{x_1, x_2, \ldots, x_{N-1}\}$ is the displacements of the original oscillators. They are linked by the linear transformation $\boldsymbol{X} = M\boldsymbol{x}$, where the transformation matrix is determined by eq. (4). If all the oscillator displacements x_j ($j = 1, \ldots, N$) are augmented by the same increment μL (μ is an integer), the relative motions remain unchanged because all the relative displacements are unchanged; however, there is an additional phase to the center-of-mass motion wave function

$$\Psi'(\boldsymbol{X}) = \exp\left(\frac{\mathrm{i}}{\hbar}P_0(X_0 + \mu L)\right)\chi(\boldsymbol{X}). \tag{9}$$

The single-valuedness condition of quantum mechanics requires $\Psi'(\boldsymbol{X}) = \Psi(\boldsymbol{X})$, which leads to the quantized total momentum (n is an integer):

$$P_0(n) = n\frac{\hbar}{R}. \tag{10}$$

The real part of the plane waves of the center-of-mass motion versus the displacement X_0 is depicted in Figure 1(c). When the quantum number n increases, the number of nodes for the real part of the center-of-mass motion wavefunction also increases.

Besides this continuous symmetry, there is a discrete symmetry due to the periodicity of the harmonic potential shown in eq. (3). When any of the displacements x_j are augmented by μL, the Hamiltonian is still unchanged. In this sense, the operation not only introduces a similar phase to the center-of-mass motion as:

$$\Psi'(\boldsymbol{X}') = \exp\left[\frac{\mathrm{i}}{\hbar}P_0(n)\left(X_0 + \frac{1}{N}\mu L\right)\right]\chi(\boldsymbol{X}'), \tag{11}$$

but also changes the displacements of the relative motions to $\boldsymbol{X}' = \boldsymbol{X} + \mu L\boldsymbol{M}_{j_0}$. Here, $\boldsymbol{M}_{j_0}$ is the column vector of the transformation matrix $\boldsymbol{M}$. If we only focus on the additional phase of the center-of-mass motion and substitute the quantized total momentum in eq. (10), the phase $\exp(\mathrm{i}2\pi n\mu/N)$ actually only has N possible values for $\mod[n\mu, N] = 0, 1, \ldots, N-1$, where $\mod[x, y]$ gives the remainder of the division of x by y. These N operations actually constitute the N elements of the C_N group. Therefore, the total system symmetry group is $U(1)\otimes C_N$.

To obtain the energy spectrum, the corresponding Schrödinger equation is taken into consideration as:

$$\hat{H}\Psi(\boldsymbol{X}) = E(n)\Psi(\boldsymbol{X}), \tag{12}$$

where the eigenenergy contains the kinetic energy of the center-of-mass motion and the energies of the relative motions as:

$$E(n, \alpha) = \frac{n^2\hbar^2}{2mNR^2} + \epsilon(\alpha). \tag{13}$$

Here, we have already substituted the quantized total momentum into the kinetic energy $P_0^2/2mN$. Since the total momentum commutes with all displacements of the relative motions, $\left[\hat{X}_k, \hat{P}_0\right] = \mathrm{i}\hbar\delta_{k,0}$, the eigenstates describing the relative motions also satisfy the following Schrödinger equation:

$$\hat{H}\chi(\boldsymbol{X}) = \epsilon\chi(\boldsymbol{X}). \tag{14}$$

Usually, the energy spectrum of the relative modes ϵ is independent of the total momentum P_0, and the coherence of the relative motion states can be maintained all the time. However, the single-valuedness condition requires the wavefunction in eq. (11) to be the same as the wavefunction in eq. (7), which leads to

$$\chi(\boldsymbol{X}) = \exp(\mathrm{i}\mu\theta_n)\chi(\boldsymbol{X} + \mu L\boldsymbol{M}_{k_0}) \tag{15}$$

with $\theta_n = 2\pi n/N$ for any $k_0 = 1, 2, \ldots, N-1$. Here, the boundary conditions in eq. (15) actually can guarantee the single-valuedness condition for any μ:

$$\begin{aligned}\chi(\boldsymbol{X}) &= \exp(\mathrm{i}\theta_n)\chi(\boldsymbol{X} + L\boldsymbol{M}_{k_0}) \\ &= \exp(\mathrm{i}2\theta_n)\chi(\boldsymbol{X} + 2L\boldsymbol{M}_{k_0}) \\ &= \ldots = \exp(\mathrm{i}\mu\theta_n)\chi(\boldsymbol{X} + \mu L\boldsymbol{M}_{k_0}).\end{aligned} \tag{16}$$

Obviously, θ_n depends on the total momentum P_0, which eventually results in the energy of the relative motions $\epsilon(n, \alpha)$ becoming dependent of the total momentum. For a different quantum number n of the total momentum, the group of energy levels forms the thin spectrum, which plays an essential role in the spontaneous decoherence. The Hamiltonian, in the first place, possesses C_N-symmetry, implying a periodic θ_n as θ_n=$\theta_{n+\mu N}$; therefore, the thin spectrum is also periodic: $\epsilon(n, \alpha) = \epsilon(n + \mu N, \alpha)$. Since the Hamiltonian has an inversion symmetry when $\boldsymbol{x} \to -\boldsymbol{x}$, this implies that the thin spectrum is an even function of n: $\epsilon(n, \alpha) = \epsilon(-n, \alpha)$.

We will solve the energy spectrum of the relative motions from its eigenequation in eq. (14) together with the nontrivial boundary conditions in eq. (15) in order to obtain the thin spectrum depending on the quantum number n of the total momentum in the next section.

3 The total energy spectrum

Since the harmonic oscillator potentials for the relative motions are still periodic, according to the Floquet theorem [37], the k-th relative motion can be rewritten as:

$$\chi_k(X_k) = \mathrm{e}^{\mathrm{i}q_k X_k} u_k(X_k) \tag{17}$$

with wave vector $\boldsymbol{q}_k$ and the periodic part $u_k(X_k)$. According to eq. (8), the total relative motions are described by the product state as:

$$\chi(\boldsymbol{X}) = \mathrm{e}^{\sum_{k=1}^{N-1}\mathrm{i}q_k X_k}\prod_{k=1}^{N-1} u_k(X_k). \tag{18}$$

In order to satisfy the boundary conditions in eq. (15), we calculate the wavefunctions of all the relative motions when the j_0-th oscillator displacement is augmented by L as:

$$\begin{aligned}&\chi\left(\boldsymbol{X} + L\boldsymbol{M}_{j_0}\right) \\ &= \mathrm{e}^{\sum_{k=1}^{N-1}\mathrm{i}q_k\left(X_k + LM_{k_0}^k\right)}\prod_{k=1}^{N-1} u_k\left(X_k + LM_{k_0}^k\right) \\ &= \mathrm{e}^{\sum_{k=1}^{N-1}\mathrm{i}q_k LM_{k_0}^k}\mathrm{e}^{\sum_{k=1}^{N-1}\mathrm{i}q_k X_k}\prod_{k=1}^{N-1} u_k\left(X_k + LM_{k_0}^k\right) \\ &= \mathrm{e}^{\sum_{k=1}^{N-1}\mathrm{i}q_k LM_{k_0}^k}\chi(\boldsymbol{X}),\end{aligned} \tag{19}$$

where $M_{k_0}^k$ are the elements of the vector $\boldsymbol{M}_{k_0} = \left(M_{k_0}^1, M_{k_0}^2, \ldots, M_{k_0}^{N-1}\right)$ and in the last step we apply the periodicity of the wavefunctions $\{u_k(X_k)\}$ as:

$$\prod_{k=1}^{N-1} u_k\left(X_k + LM_{k_0}^k\right) = \prod_{k=1}^{N-1} u_k(X_k). \tag{20}$$

In contrast with the boundary conditions in eq. (15), we actually obtain the constraints for the wave vectors $\{\boldsymbol{q}_k\}$:

$$\sum_{k=1}^{N-1} LM_{k_0}^k \boldsymbol{q}_k + \theta_n = 0, \tag{21}$$

which should be satisfied for any k_0. The $N-1$ constraints completely determine the wave vectors $\{\boldsymbol{q}_k\}$. In vector form, they can be rewritten as:

$$L\boldsymbol{M}\boldsymbol{q} + \theta_n\boldsymbol{I} = 0, \tag{22}$$

where $\boldsymbol{q} = (q_1, q_2, \ldots, q_{N-1})^{\mathrm{T}}$ and $\boldsymbol{I} = (1, 1, \ldots, 1)^{\mathrm{T}}$. The solution is straightforwardly obtained as (see Appendix A1):

$$q_j = \begin{cases} q, & 1 \le k \le \frac{N-1}{2}, \\ 0, & \frac{N+1}{2} \le k \le N-1, \end{cases} \tag{23}$$

for odd N and

$$q_j = \begin{cases} q, & 1 \le k \le \frac{N}{2} - 1, \\ \frac{q}{2}, & k = \frac{N}{2}, \\ 0, & \frac{N}{2} + 1 \le k \le N-1, \end{cases} \tag{24}$$

for even N, with $q = \frac{\sqrt{2}n}{\sqrt{N}R}$. It indicates that for those relative motions with $k < N/2$ the wave vectors $\boldsymbol{q}$ are exactly same, which are proportional to the quantum number n as well as the total momentum $P_0(n)$, while for relative motions with $k > N/2$ the wave vectors vanish. In this sense, the phase factor θ_n resulting from the total momentum is now divided into individual phase factors of those relative motions with $k \le N/2$. In fact, the consequence of the nontrivial boundary conditions is an additional phase factor in eq. (15), which is actually equivalent to introducing a gauge field to the relative motions (see Appendix A2).

Therefore, it is feasible to deal with a single relative motion in order to obtain the corresponding energy spectrum

once the individual periodicity of the relative motion is determined. When the j_0-th oscillator's displacement is augmented by μL, the change in the relative motion displacement is $\boldsymbol{X}' = \boldsymbol{X} + \mu L \boldsymbol{M}_{k_0}$ and the periodic part of the wavefunction $u_k(X_k)$ satisfies

$$u_k(X_k) = u_k\left(X_k + LM_{k_0}^k\right). \tag{25}$$

Since we can permutate the indices of the original oscillators such that $\{k_0, k_0+1, \ldots, N, 1, 2, \ldots, k_0-1\} \to \{1, 2, \ldots, N\}$ in order to always augment the first oscillator's displacement, the periodicities of those relative motions are considered to be $u_k(X_k) = u_k\left(X_k + LM_1^k\right)$. In this sense, we can solve the Schrödinger equation

$$\hat{H}_k \chi_k(X_k) = \epsilon_k \chi_k(X_k), \tag{26}$$

and the corresponding boundary conditions, which require both the wavefunction and the derivative of the wavefunction to be continuous, as:

$$\chi_k\left(-\frac{L}{2}M_1^k\right) = \mathrm{e}^{\mathrm{i}q_k L M_1^k}\chi_k\left(\frac{L}{2}M_1^k\right), \tag{27a}$$

$$\frac{\mathrm{d}}{\mathrm{d}X_k}\chi_k(X_k)\Big|_{X_k=-\frac{L}{2}M_1^k} = \mathrm{e}^{\mathrm{i}q_k L M_1^k}\frac{\mathrm{d}}{\mathrm{d}X_k}\chi_k(X_k)\Big|_{X_k=\frac{L}{2}M_1^k}. \tag{27b}$$

The energy spectrum depending on the quantum number n can be approximated as (see Appendix A3):

$$\epsilon_k(n,\alpha) = \left(\frac{1}{2} + \alpha + \delta_k(n,\alpha)\right)\hbar\omega_k \tag{28}$$

with the frequency of the oscillator of the k-th relative motion $\omega_k = 4\sqrt{\kappa/m}\sin(\pi k/N)$. The explicit form of the total momentum-dependent term $\delta_k(n,\alpha)$ can be found in Appendix A3.

The total thin spectrum is the sum of all the energies of the relative motions: $\epsilon(n,\alpha) = \sum_{k=1}^{N-1}\epsilon_k(n,\alpha)$. The schematics of the spectrum are depicted in Figure 2, which is almost quadratic in n and linear in α. The subtle difference between the different thin spectra with different excitation quantum numbers of the relative modes α usually still depends on the total momentum, which leads to the decoherence of the relative modes. The details of this decoherence process will be discussed in the next section.

4 Decoherence of the relative motions

4.1 Decoherence factor

To explore the decoherence of the relative modes caused by the thin spectrum, we consider the dynamics of an actual qubit of the multiparticle system. The qubit is chosen to be

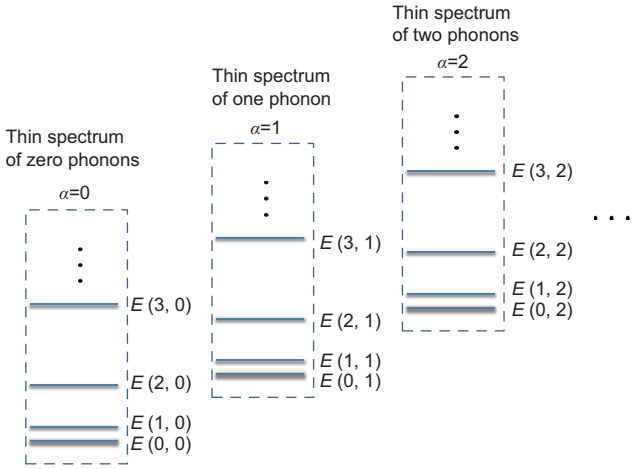

Figure 2 (Color online) Schematic illustration of the total energy spectrum $E(n,\alpha)$. The thin spectrum is almost quadratic in the quantum number n of the total momentum, and linear in the quantum number α of the relative motions.

$(a|0\rangle + b|1\rangle)\otimes|n\rangle$, with the ground state of the relative modes $|\alpha=0\rangle$, the first excitation state of the relative modes $|\alpha=1\rangle$, and the center-of-mass state $|n\rangle$ (Figure 2). If the multiparticle system condenses into the BEC (Bose-Einstein condensate) state with a single momentum, which is equivalent to $|n\rangle$ only containing a single mode plane wave, the effect of the thin spectrum is adding a phase factor to the off-diagonal elements of the relative modes' reduced density matrix, and thus no decoherence occurs. However, at a relatively high temperature such as $k_\mathrm{B}T \gg \hbar^2/2mNR^2$, the center-of-mass state usually stays in the thermal state

$$\rho_T = \frac{1}{Z}\sum_{n=-\infty}^{\infty}\mathrm{e}^{-\beta E(n,\alpha)}|n\rangle\langle n| \tag{29}$$

for a macroscopic object with $\beta^{-1} = k_\mathrm{B}T$, where the thin spectrum is labeled by the quantum numbers n of the total momentum and α of the relative motions:

$$E(n,\alpha) = \frac{n^2\hbar^2}{2mNR^2} + \epsilon(n,\alpha), \tag{30}$$

and $Z = \sum_n \mathrm{e}^{-\beta E(n,0)}$ is the partition function corresponding to the product of the center-of-mass thermal state and the ground state of the relative modes.

We prepare the initial state of the qubit in its ground state $|0\rangle$ and then apply a rotation to transform the ground state into $a|0\rangle + b|1\rangle$. In this case, the initial density matrix is the product of the thermal state density matrix and the qubit one:

$$\begin{aligned}\boldsymbol{\rho}_0 =& \boldsymbol{\rho}_T \otimes \boldsymbol{\rho}_Q \\ =& \frac{1}{Z}\sum_{n=-\infty}^{\infty}\mathrm{e}^{-\beta E(n,0)}|n\rangle\langle n| \\ & \times (a|0\rangle + b|1\rangle)(a^*\langle 0| + b^*\langle 1|).\end{aligned} \tag{31}$$

Since we have solved the total energy spectrum of the system, the time evolution of the eigenstate $|n,\alpha\rangle \equiv |n\rangle\otimes|\alpha\rangle$ ($\alpha = 0, 1$) can be described by a time evolution operator:

$$U_t|n,\alpha\rangle = \exp\left[-\frac{\mathrm{i}}{\hbar}E(n,\alpha)t\right]|n,\alpha\rangle. \tag{32}$$

Then, the time evolution of the density matrix is

$$\begin{aligned}\boldsymbol{\rho}_t =& U_t\boldsymbol{\rho}_0 U_t^{\dagger}\\ =&\frac{1}{Z}\sum_{n=-\infty}^{\infty}\mathrm{e}^{-\beta E(n,0)}|n\rangle\langle n|\Big(|a|^2|0\rangle\langle 0| + |b|^2|1\rangle\langle 1|\\ &+a^*b\mathrm{e}^{-\frac{\mathrm{i}}{\hbar}(E(n,1)-E(n,0))t}|1\rangle\langle 0| + h.c.\Big).\end{aligned} \tag{33}$$

Tracing out the degree of freedom of the center-of-mass, we can define the decoherence factor from the coefficients of the off-diagonal elements as:

$$F = \left|\frac{1}{Z}\sum_{n=-\infty}^{\infty}\mathrm{e}^{-\beta E(n,0)}\mathrm{e}^{-\frac{\mathrm{i}}{\hbar}\Delta E(n)t}\right|, \tag{34}$$

with $\Delta E(n) = E(n,1) - E(n,0)$. Obviously, the decoherence factor is equal to or less than 1, which characterizes the completeness of the decoherence. $F = 1$ means the state has the same coherence as the initial quantum state; $F < 1$ means decoherence occurs, and the multiparticle system becomes classical when $F = 0$.

4.2 Timescale of the decoherence at two limits

Since the ground state is the product of the ground states of all relative motions, namely $|0\rangle = \prod_{k=1}^{N-1}\otimes|0_k\rangle$, the ground state energy

$$E(n,0) = \frac{n^2\hbar^2}{2mNR^2} + \sum_{k=1}^{N-1}\left(\frac{1}{2}+\delta_k^n\right)\hbar\omega_k \tag{35}$$

is the summation of the ground state energies of all relative motions and the kinetic energy of the center-of-mass motion. Additionally, since the first excited state is the state where the $(N-1)$ relative motions remain in the ground state and only the first relative motion is excited to the excited state as $|1\rangle = |1_1\rangle\prod_{k=2}^{N-1}\otimes|0_k\rangle$, the energy difference in the decoherence factor actually only depends on the energy level spacing of the ground state and the excited state of the first relative motion, namely

$$\begin{aligned}&\Delta E(n) = \epsilon_1(n,1) - \epsilon_1(n,0)\\ &\approx -\hbar\omega_1\frac{g}{2}\cos\left(4\pi\frac{n}{N}\right),\end{aligned} \tag{36}$$

where $g\hbar\omega_1 = \Delta E(N/4) - \Delta E(0)$ is the maximum energy difference between thin spectra. Here, we have assumed the thin spectrum has cosine-type oscillating behavior because it is a periodic even function associated with the period $N/2$ of the phase factor θ_n. Under this approximation, the decoherence factor in eq. (34) can be written in terms of a series of Bessel functions:

$$\begin{aligned}F \approx& \left|\frac{1}{Z}\int_{-\infty}^{\infty}\mathrm{e}^{-\beta\Delta_e' n^2}\mathrm{e}^{\mathrm{i}\frac{g}{2}\omega_1 t\cos\left(4\pi\frac{n}{N}\right)}\mathrm{d}n\right|\\ =&\left|\frac{1}{Z}\int_{-\infty}^{\infty}\mathrm{e}^{-\beta\Delta_e' n^2}\sum_{\gamma=-\infty}^{\infty}\mathrm{e}^{\mathrm{i}\alpha\left(4\pi\frac{n}{N}+\frac{\pi}{2}\right)}J_\gamma\left[\frac{g}{2}\omega_1 t\right]\mathrm{d}n\right|\\ =&\left|\sum_{\gamma=-\infty}^{\infty}J_\gamma\left(\frac{g}{2}\omega_1 t\right)\mathrm{e}^{\mathrm{i}\gamma\frac{\pi}{2}}\exp\left(-\frac{4\pi^2\gamma^2}{N^2\beta\Delta_e'}\right)\right|.\end{aligned} \tag{37}$$

Here, we have assumed the second term in $E(n,0)$ is quadratic in n as $\sum_{k=1}^{N-1}\delta_k^n\hbar\omega_k = \Delta_e n^2$ and $\Delta_e' = \Delta_e + \hbar^2/2mNR^2$. We also have neglected the n-independent terms because they will vanish in the absolute value of eq. (34).

Obviously, for the first limit, if $4\pi^2/N^2\beta\Delta_e' \gg 1$ the last term exponentially decays as γ increases and eventually only the $\gamma = 0$ term contributes to the decoherence factor as $F = J_0\left(\frac{g}{2}\omega_1 t\right)$. In this limit, the decoherence factor is independent of the temperature and has an oscillating behavior associated with the 0-th Bessel function.

We can obtain the decoherence factor in another limit. Since the decoherence factor in eq. (34) is basically the integral of both the Gaussian part and the dynamic phase; if the period of the dynamic phase ($N/2$) is greater than the full width at half maximum (FWHM) of the Gaussian part, only the first period of the thin spectrum contributes to the decoherence factor. In this sense, the energy difference is approximately linear:

$$\begin{aligned}\Delta E(n) =& \epsilon_1(n,1) - \epsilon_1(n,0)\\ \approx&\frac{\Delta_g}{N}|n|\hbar\omega_k\end{aligned} \tag{38}$$

with $\Delta g = g_1(1,1) - g_1(1,0)$. The definition of function $g_1(k,m)$ can be found in Appendix A3. The decoherence factor actually possesses an exponentially decaying behavior as given by

$$\begin{aligned}F \approx& \left|\frac{1}{Z}\int_{-\infty}^{\infty}\mathrm{e}^{-\beta\Delta_e' n^2}\mathrm{e}^{-\mathrm{i}\sqrt{\frac{\kappa}{m}}2\pi\frac{\Delta_g}{N^2}|n|t}\mathrm{d}n\right|\\ =&\mathrm{e}^{-\left(\frac{t}{\tau}\right)^2}\sqrt{1+\mathrm{Erfi}\left(\frac{t}{\tau}\right)^2},\end{aligned} \tag{39}$$

where

$$\tau = \sqrt{\frac{\beta N^4 m\Delta_e'}{\pi^2\Delta_g^2\kappa}}, \tag{40}$$

Erfi(t/τ) is the imaginary error function and the summation becomes an integral at high temperatures, such as $k_{\mathrm{B}}T \gg \hbar^2/2mNR^2$. The typical timescale of the decoherence is

$$\tau_{\mathrm{spon}} = \sqrt{\frac{2(\pi-2)}{\pi}}\tau \approx 0.85\tau. \tag{41}$$

Since the Δ_e and Δ_g usually depend on all other parameters such as N, T, κ, m, and R (see Appendix A3), it is hard to determine the exact dependence of the decoherence factor on those parameters, and we will present the numerical analysis in the next subsection. In particular, if the lattice constant R/N is unchanged while the ring container radius R increases, the decoherence time tends to infinity, Δ_e and Δ_g both tend to remain constant, and thus the τ_{spon} is proportional to $\sqrt{R}$. This implies that no spontaneous decoherence occurs in the thermodynamic limit.

4.3 Numerical results

The numerical calculations based on eq. (34) are presented in this section. The typical thin spectrum $\epsilon_1(n,0)$ for zero phonons of the first relative motion and the normalized Gaussian part

$$P(n) = \frac{1}{Z}\mathrm{e}^{-\beta\left(\frac{n^2\hbar^2}{2mNR^2}\right)} \tag{42}$$

in the decoherence factor versus the quantum number n are depicted in Figure 3(a) and (b). The parameters are chosen to be $N = 80$, $R = 0.5$ μm, $\kappa = 10^{-13}$ N/s, $m = 40m_{\mathrm{p}}$, with m_{p} the mass of the proton. The temperature is $T = 0.1$ μK for (a) and $T = 8$ μK for (b). This mechanism is depicted in Figure 3(c) and (d), where each successive complex term in the summation of the decoherence factor is regarded as a vector. In this sense of the vector summation picture, the decoherence factor is the length of the vector summation. There are three typical decoherence processes. If all the phases of the vectors are the same, the coherence can be maintained well. If $N/4$ is larger than the full width at the half-maximum of the Gaussian part, only the first period of the thin spectrum contributes to the decoherence factor shown in Figure 3(a) and (c). When $N/4$ is smaller than the FWHM of the Gaussian part, the next several periods of the thin spectrum also contribute to the decoherence factor, and it will usually extend the decoherence time shown in Figure 3(b) and (d). Usually, the FWHM of the Gaussian part

$$n_{\mathrm{FWHM}} = \sqrt{\frac{2mNR^2}{\beta\hbar^2}} \tag{43}$$

decreases when the temperature T, the particle mass m, the particle number N, and the radius of the ring container R decrease. In this sense, we can define one parameter

$$r = \frac{n_{\mathrm{FWHM}}}{N/4} = 4\sqrt{\frac{2mR^2}{\beta N\hbar^2}} \tag{44}$$

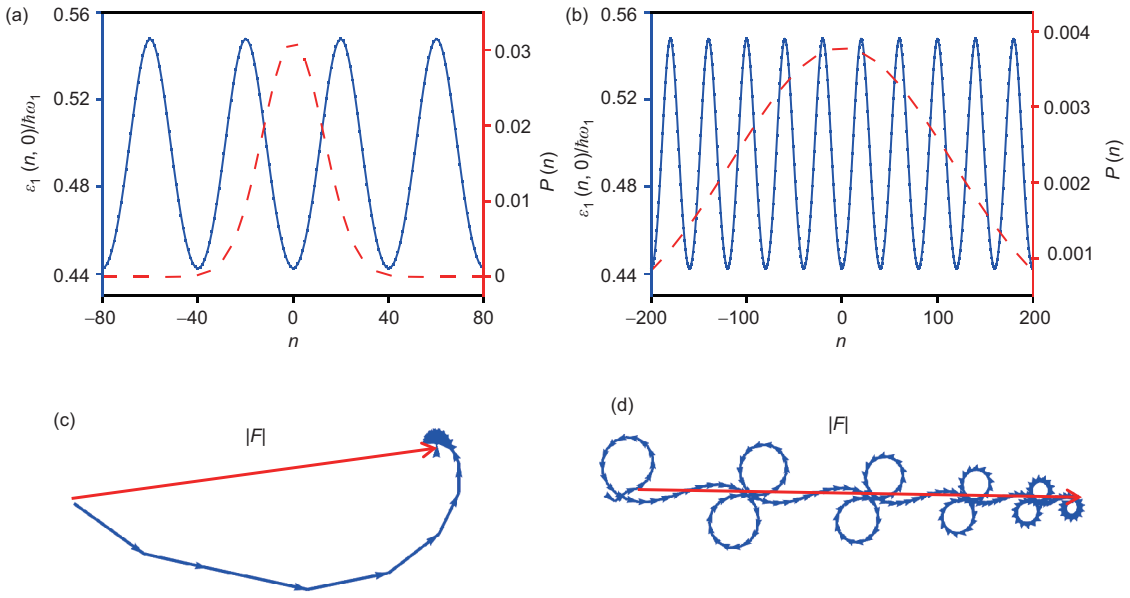

Figure 3 (Color online) (a) and (b) Typical thin spectrum $\epsilon_1(n,0)$ for zero phonons of the first relative motion, and the normalized Gaussian part $P(n)$ versus the quantum number n. The blue solid line and the red dashed line represent $\epsilon_1(n,0)$ and $P(n)$, respectively. The parameters are chosen to be $N = 80$, $R = 0.5$ μm, $\kappa = 10^{-13}$ N/s, $m = 40m_{\mathrm{p}}$, where m_{p} is the mass of the proton. The temperature is $T = 0.1$ μK for (a) and $T = 8$ μK for (b); (c) and (d) typical vector summation pictures of the decoherence factor $|F|$, respectively corresponding to the cases (a) and (b). The red arrow and the blue arrows respectively represent the decoherence factor $|F|$ and successive terms in the decoherence factor. Obviously, for case (a) there is only the single period of the thin spectrum contributing to the decoherence factor. For the case (b), there are multiple periods of the thin spectrum contributing to the decoherence factor.

to distinguish between these two cases, where $r < 1$ and $r > 1$ respectively correspond to the single and multi-period contributions shown in Figure 3(a) and (b).

Eq. (36) is valid for describing the decoherence process when the thin spectrum has approximately cosine-type oscillating behavior. The decoherence factor obtained from eq. (34) and the approximate decoherence factor in eq. (37) are shown in Figure 4(a) with solid lines and dashed lines, respectively. For the summation of the series of Bessel functions in eq. (37), we need to set a cutoff for γ. Here, we set a parameter

$$\eta = \frac{4\pi^2}{N^2\beta\Delta_e'} \tag{45}$$

to determine the cutoff:

$$\exp\left(-\eta\gamma_{\text{cutoff}}^2\right) = 10^{-2}. \tag{46}$$

The parameters are chosen to be $N = 80$, $\kappa = 10^{-13}$ N/s, $R = 0.5$ μm, $m = 40m_{\text{p}}$. The temperatures are, respectively, $T = 483, 121, 31$ nK to guarantee $r = 0.5, 1, 2$ for the red, blue, and purple lines, and the cutoff $\gamma_{\text{cutoff}} = 9, 5, 3$ for the red, blue, and purple dashed lines respectively. The approximate solution describes the decoherence process quite well for the low temperature case, where only a few Bessel functions are contributing to the oscillating behavior of the decoherence factor.

For the relatively high temperature case, such as $r < 1$, eq. (39) is valid to describe the decoherence process. The exact decoherence factor obtained from eq. (34) and the approximate decoherence factor in eq. (39) are shown in Figure 4(b) with solid lines and dashed lines, respectively. The parameters are the same as the ones used for Figure 4(a). The decoherence processes for short timescales can be described quite well by eq. (39), while the long-term behavior deviates from the approximate solution because of the linear dependence of the energy difference we assumed in eq. (38). For $\gamma > 1$, the multi-period contributions introduce oscillating behavior into the decoherence factor.

Besides the temperature, the decoherence time can be extended by adjusting other parameters such as the particle number N, spring constant κ, radius of the ring container R, and the particle mass m. The numerical calculation directly based on the exact solution is shown in Figure 5. The basic parameters are chosen to be $N = 80$, $T = 10^{-5}K$, $\kappa = 10^{-13}$ N/s, $R = 1$ μm, $m = 4m_{\text{p}}$ where m_{p} is the mass of the proton. From Figure 5(a)–(e), the evolutions of the decoherence factor are depicted for different particle numbers N, temperatures T, spring constants κ, radii of the ring container R, and particle masses m. The spontaneous decoherence occurs at first, and it is possible for the decoherence factor to rebound to a relative large value at a later time. In some cases the rebound can reach a value of almost 1, as shown in Figure 5(b). Such a rebound of the decoherence factor results from the contributions from different periods shown in Figure 3(d), which possibly cancel each other and eventually prolong the decoherence time. If we define the decoherence time as the time before the first possible rebound, it is obviously extended when decreasing the particle number and the temperature, or increasing the spring constant, the ring container radius, and the particle mass. Intriguingly, if the linear mass density $\eta = N/2\pi R$ is kept unchanged and the particle number increases just as shown in Figure 5(f), the decoherence time is extended instead of shortened when only the particle number is increased, as shown in Figure 5(a). It implies that the spontaneous decoherence does not occur at the thermodynamic limit.

5 Conclusion

We studied the spontaneous decoherence of coupled harmonic oscillators confined in a ring container, where the

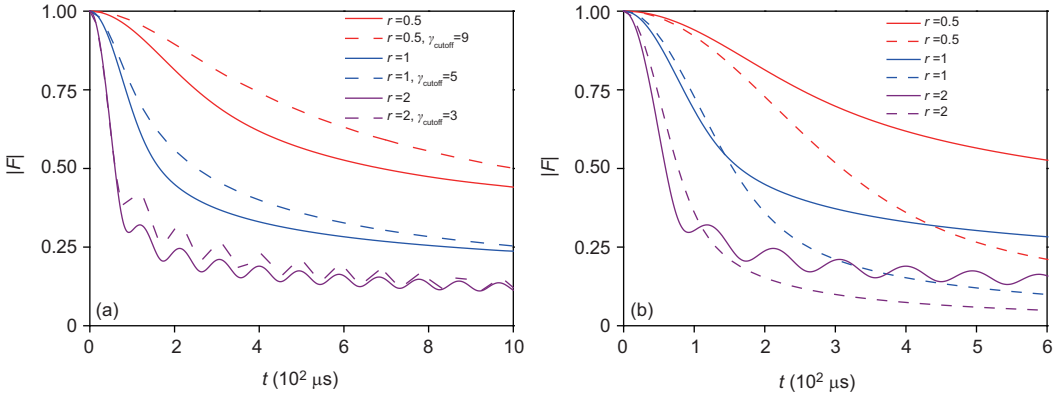

Figure 4 (Color online) Decoherence factor obtained by the exact solution (solid lines) and the approximate solution (dashed lines) based on eq. (37) (a) and eq. (39) (b). The parameters are chosen to be $N = 80$, $\kappa = 10^{-13}$ N/s, $R = 0.5$ μm, $m = 40m_{\text{p}}$. The temperatures are, respectively, $T = 483, 121, 31$ nK to guarantee $r = 0.5, 1, 2$ for red, blue, and purple lines, respectively. The cutoff is $\gamma_{\text{cutoff}} = 9, 5, 3$ for red, blue, and purple dashed lines, respectively.

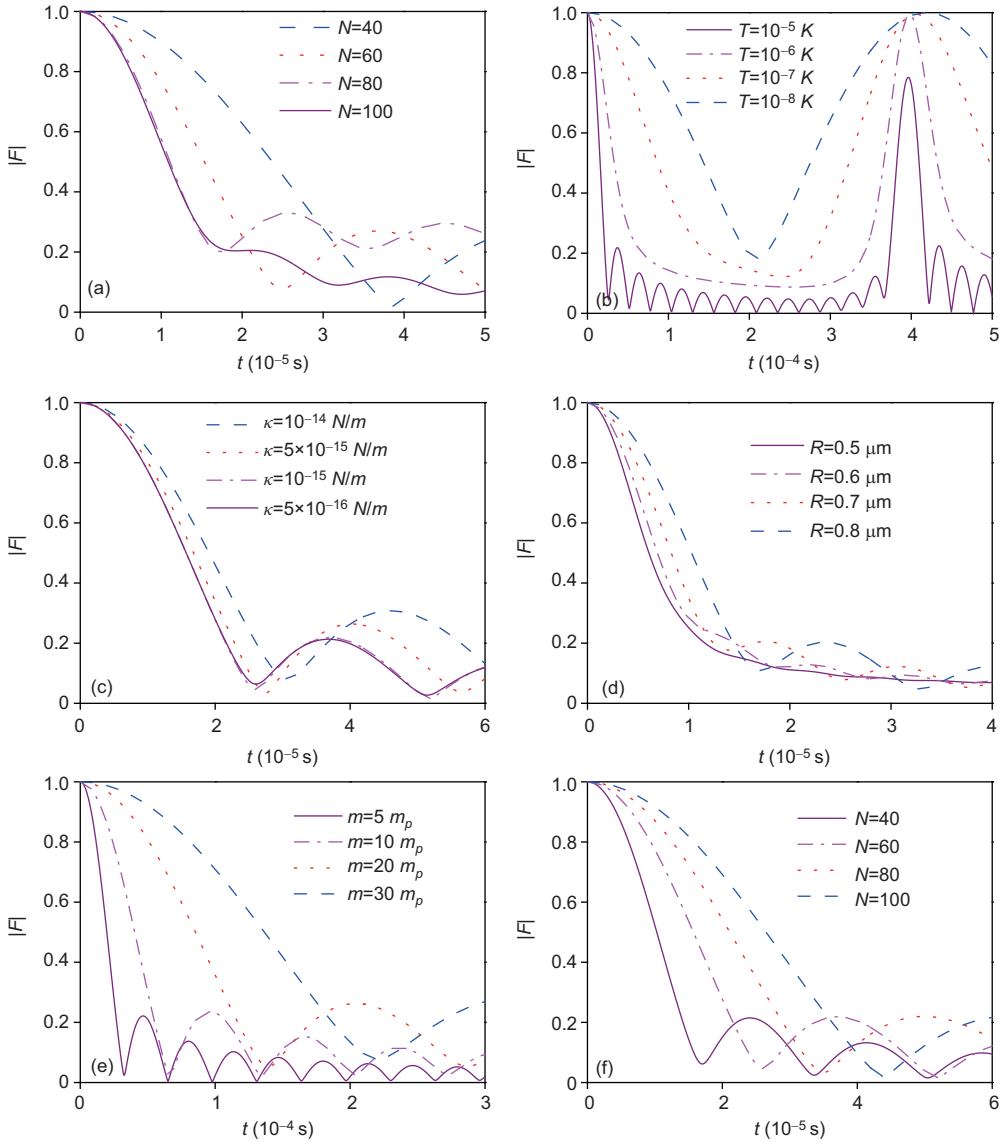

Figure 5 (Color online) Evolutions of the decoherence factor for different (a) particle numbers N, (b) temperatures T, (c) spring constants κ, (d) radii of the ring container R, and (e) particle masses m. For (f), the particle number N and the ring container R are increased simultaneously in order to keep the linear mass density $\eta = N/2\pi R$ unchanged. The basic parameters are chosen to be $N = 80$, $T = 10^{-5}$ K, $\kappa = 10^{-13}$ N/s, $R = 1$ μm, $m = 4m_{\rm p}$, with $m_{\rm p}$ the mass of the proton. Basically, the decoherence time is extended for smaller particle numbers, lower temperatures, stronger spring constants, larger ring containers, and heavier particles. If the linear mass density $\eta = N/2\pi R \approx 9.55 \times 10^6$ m^{-1} is kept unchanged and the particle number increased, the decoherence time is extended instead of shortened when only the particle number is increased, as shown in (a). It implies that the spontaneous decoherence does not occur at the thermodynamic limit.

nearest-neighbor harmonic potentials are taken into consideration. Without any surrounding environment, the quantum superposition state prepared in the relative degrees of freedom gradually loses its quantum decoherence. We study the spontaneous decoherence existing as in a closed multiparticle system where the symmetry is not broken.

The multiparticle system we study actually possesses $U(1) \otimes C_{\rm N}$-symmetry. The Hamiltonian can be divided into the center-of-mass motion part and the relative motion parts. The harmonic potentials between the oscillators are periodic because of the ring configuration. Then, nontrivial boundary conditions emerge to guarantee the single-valuedness of the wave function, which eventually results in the total energy spectrum not only depending on the excitations of the relative motion, but also on the total momentum corresponding to the center-of-mass motion. The consequence of the nontrivial boundary conditions is an additional phase factor in eq. (15), which is actually equivalent to introducing a gauge field to the relative motions. There is a thin spectrum of the total momentum that contributes to the decoherence process. If the center-of-mass motion is not condensed to the state with a single momentum, spontaneous decoherence occurs in the

superposition states of the relative motions. Since there is no environment or symmetry-breaking field, the decoherence in our model is definitely spontaneous.

This spontaneous decoherence is interpreted as the gauge coupling between the center-of-mass and relative degrees of freedoms. The paradox that the information represented by the coherence is always lost in a closed system can be explained by the infinite degrees of freedom of the center-of-mass motion acting like a heat bath. Certainly, the roles of the center-of-mass motion and the relative motions can be switched. With proper initial preparation, the degrees of freedom of the relative motions can be regarded as the thermal bath as well, and eventually cause the decoherence of the states prepared in the center-of-mass motion. In particular, the spontaneous decoherence is completely missing at the thermodynamic limit because the nontrivial boundary conditions become the trivial Born-von Karman boundary condition. Our investigation shows that a thermal macroscopic object with certain symmetries has a chance to for its quantum properties to degrade even without applying an external symmetry-breaking field or a surrounding environment.

This work was supported by the National Natural Science Foundation of China (Grant Nos. 11504241, and 11374032), the National Key Basic Research Program (Grant No. 2014CB848700), and the Natural Science Foundation of Shenzhen University (Grants No. 201551). The authors thank Professor HongChen Fu of Shenzhen University for helpful discussions.

1 W. H. Zurek, Phys. Today **44**, 36 (1991).
2 S. Haroche, Phys. Today **51**, 36 (1998).
3 W. H. Zurek, Rev. Mod. Phys. **75**, 715 (2003).
4 C. H. Bennett, and D. P. DiVincenzo, Nature **404**, 247 (2000).
5 H. T. Quan, P. Zhang, and C. P. Sun, Phys. Rev. E **73**, 036122 (2006).
6 T. Shi, Y. Li, Z. Song, and C. P. Sun, Phys. Rev. A **71**, 032309 (2005).
7 B. Chen, and Z. Song, Sci. China-Phys. Mech. Astron. **53**, 1266 (2010).
8 B. Chen, and Y. Li, Sci. China-Phys. Mech. Astron. **59**, 640302 (2016).
9 D. A. Lidar and T. A. Brun, *Quantum Error Correction* (Cambridge University Press, Cambridge, 2013), p. 3.
10 D. Howard, Philosophy. Sci. **71**, 669 (2004).
11 E. Joos, and H. D. Zeh, Z. Physik B-Condensed Matt. **59**, 223 (1985).
12 H. D. Zeh, Found. Phys. **1**, 69 (1970); Found. Phys. **3**, 109 (1973); H. D. Zeh, Phys. Lett. A **172**, 189 (1993).
13 W. H. Zurek, Phys. Rev. D **24**, 1516 (1981); W. H. Zurek, Phys. Rev. D **26**, 1862 (1982); W. H. Zurek, Prog. Theor. Phys. **89**, 281 (1993).
14 D. L. Zhou, P. Zhang, and C. P. Sun, Phys. Rev. A **66**, 012112 (2002).
15 C. P. Sun, Phys. Rev. A **48**, 898 (1993).
16 W. H. Zurek, and J. P. Paz, Phys. Rev. Lett. **72**, 2508 (1994).
17 C. P. Sun, D. L. Zhou, S. X. Yu, and X. F. Liu, Eur. Phys. J. D **13**, 145 (2001); C. P. Sun, X. F. Liu, D. L. Zhou, and S. X. Yu, Eur. Phys. J. D **17**, 85 (2001); C. P. Sun, X. F. Liu, D. L. Zhou, and S. X. Yu, Phys. Rev. A **63**, 012111 (2000).
18 H. D. Zeh, *The Physical Basis of the Direction of Time* (Springer, Berlin, 4th ed, 2001), p.101.
19 E. Joos, H. D. Zeh, C. Kiefer, D. Giulini, J. Kupsch, and I.-O. Stamatescu, *Decoherence and the Appearance of a Classical World in Quantum Theory* (Springer, NewYork, 2nd ed, 2003), p. 35.
20 M. Schlosshauer, Rev. Mod. Phys. **76**, 1267 (2005).
21 F. Xue, S. X. Yu, and C. P. Sun, Phys. Rev. A **73**, 013403 (2006).
22 G. Rempe, S. Dürr, and T. Nonn, Nature **395**, 33 (1998).
23 M. Arndt, O. Nairz, J. Vos-Andreae, C. Keller, G. van der Zouw, and A. Zeilinger, Nature **401**, 680 (1999).
24 R. Omnès, *The Interpretation of Quantum Mechanics*, (Princeton University Press, Princeton, 1994), p. 291.
25 P. Zhang, X. F. Liu, and C. P. Sun, Phys. Rev. A **66**, 042104 (2002).
26 J. van Wezel, J. van den Brink, and J. Zaanen, Phys. Rev. Lett. **94**, 230401 (2005).
27 J. van Wezel, J. Zaanen, and J. van den Brink, Phys. Rev. B **74**, 094430 (2006).
28 J. van Wezel, Phys. Rev. B **78**, 054301 (2008).
29 J. van Wezel, and J. van den Brink, Phys. Rev. B **77**, 064523 (2008).
30 H. T. Quan, Z. Song, X. F. Liu, P. Zanardi, and C. P. Sun, Phys. Rev. Lett. **96**, 140604 (2006).
31 I. Pikovski, M. Zych, F. Costa, and C. Brukner, Nat. Phys. **11**, 668 (2015).
32 I. Pikovski, M. Zych, F. Costa, and C. Brukner, arXiv: 1508.03296.
33 C. Gooding, and W. G. Unruh, Found Phys **45**, 1166 (2015).
34 N. Byers, and C. N. Yang, Phys. Rev. Lett. **7**, 46 (1961).
35 R. Resta, Phys. Rev. Lett. **80**, 1800 (1998).
36 R. Peierls, *Surprises in Theoretical Physics* (Princeton University Press, Princeton, 1979), p. 14.
37 W. Magnus, S. Winkler. *Hill's Equation* (Dover-Phoenix Editions, New York, 2004) p. 3.
38 H. E. Montgomery Jr., G. Campoy, and N. Aquino, arXiv: 0803.4029.
39 O. Kübler, and H. D. Zeh, Ann. Phys. **76**, 405 (1973).

Appendix

Appendix A1 Wave vector solutions

To obtain the wave vectors $\boldsymbol{q} = (q_1, q_2, \ldots, q_{N-1})^{\mathrm{T}}$, we need to solve eq. (22). Here, $\boldsymbol{I} = (1, 1, \ldots, 1)^{\mathrm{T}}$ and $L = 2\pi R$ is the perimeter of the ring container. The matrix $\boldsymbol{M}$ in eq. (22) is determined by the Fourier transformation as eq. (4). Both the explicit forms of $\boldsymbol{M}$ for odd and even N can be written together as:

$$\boldsymbol{M} = \sqrt{\frac{2}{N}} \begin{bmatrix} A & B \\ A^* & B^* \end{bmatrix}. \tag{a1}$$

Taking the odd N case as an example, the block matrices are, respectively,

$$\boldsymbol{A} = \begin{bmatrix} C_1 \\ C_2 \\ \vdots \\ C_{\frac{N-1}{2}} \end{bmatrix}, \quad \boldsymbol{A}^* = \begin{bmatrix} C_{\frac{N-1}{2}} \\ C_{\frac{N-3}{2}} \\ \vdots \\ C_1 \end{bmatrix}, \tag{a2a}$$

$$\boldsymbol{B} = \begin{bmatrix} S_1 \\ S_2 \\ \vdots \\ S_{\frac{N-1}{2}} \end{bmatrix}, \quad \boldsymbol{B}^* = -\begin{bmatrix} S_{\frac{N-1}{2}} \\ S_{\frac{N-3}{2}} \\ \vdots \\ S_1 \end{bmatrix}, \tag{a2b}$$

with row vectors

$$\boldsymbol{C}_n = \left[\cos(n\phi)\ \cos(2n\phi)\ \cdots\ \cos\left(\left(\tfrac{N-1}{2}\right)n\phi\right)\right], \tag{a3a}$$

$$\boldsymbol{S}_n = \left[-\sin\left(\left(\tfrac{1}{2}+n\right)\phi\right)\ \sin\left(2\left(\tfrac{1}{2}+n\right)\phi\right)\right.$$
$$\left.\cdots\ (-1)^{\left(\frac{N-1}{2}\right)}\sin\left(\left(\tfrac{N-1}{2}\right)\left(\tfrac{1}{2}+n\right)\phi\right)\right], \tag{a3b}$$

$(n = 1, 2, \ldots, \frac{N-1}{2})$ and $\phi = 2\pi/N$. According to the identities

$$\sum_{n=1}^{\frac{N-1}{2}} \cos(nj\phi) = \text{const.} \tag{a4}$$

for any $j = 1, 2, \ldots, \frac{N-1}{2}$ and the fact that the wave vectors $\boldsymbol{q} = (q_A, q_B)^{\mathrm{T}}$ can be divided into two parts according to the dimension of the block matrices, the only possible solution is $\boldsymbol{q}_A = (q, q, \ldots, q)^{\mathrm{T}}$ and $\boldsymbol{q}_B = (0, 0, \ldots, 0)^{\mathrm{T}}$. Therefore, eq. (22) can be simplified as:

$$qL\sqrt{\frac{2}{N}}\sum_{n=1}^{\frac{N-1}{2}}\cos(nm\phi) + \frac{2\pi n}{N} = 0, \tag{a5}$$

from which we find the solution $q = \frac{\sqrt{2}n}{\sqrt{N}R}$.

The same procedure can be applied to the even N case, and the solution is a little different from the odd N case: $\boldsymbol{q}_A = (q, q, \ldots, q, q/2)^{\mathrm{T}}$ and $\boldsymbol{q}_B = (0, 0, \ldots, 0)^{\mathrm{T}}$.

Appendix A2 Effective gauge fields on relative motions

The total momentum actually plays the role of an effective gauge field on the relative motions. Starting from the wavefunction obeying the Floquet theorem, eq. (17), the original Schrodiger equation for the k-th relative motion

$$H_k\chi_k(X_k) = \epsilon_k\chi_k(X_k) \tag{a6}$$

can be transformed into the Schrödinger equation of the periodic part as:

$$H_k^{\mathrm{eff}}u_k(X_k) = \epsilon_k u_k(X_k), \tag{a7}$$

with the exactly same eigenenergy ϵ_k. Here, the effective Hamiltonian is obtained by a unitary transformation of the original one as:

$$H_k^{\mathrm{eff}} = \mathrm{e}^{-\mathrm{i}q_kX_k}H_k\mathrm{e}^{\mathrm{i}q_kX_k}$$
$$= \frac{(P_k+\hbar q_k)^2}{2m} + \frac{\kappa}{2}\left(2\sin\frac{\pi k}{N}\right)^2 X_k^2. \tag{a8}$$

Apparently the wave vector $\boldsymbol{q}_k$ shifts the momentum of the relative motion, which is equivalent to a $U(1)$ gauge field. Since the wave vector $\boldsymbol{q}_k$ linearly depends on the quantum number n as well as the total momentum P_0, such gauge fields on the relative motions result exactly from the nonzero total momentum of the system.

Appendix A3 Energy spectrum of the periodic harmonic oscillator

The Schrödinger equation of the k-th relative motion given in eq. (26) is described by a periodic harmonic oscillator with periodicity

$$\chi_k\left(X_k + LM_1^k\right) = \mathrm{e}^{\mathrm{i}q_kLM_1^k}\chi_k(X_k). \tag{a9}$$

The basic idea to solve the energy spectrum in a periodic potential is solving the Schrödinger equation in a period and its adjacent period; then, the wavefunctions at the interface of these two periods should satisfy the continuity condition eq. (27).

The wavefunction of the k-th relative mode is the linear combination of the two degenerate Kummer or confluent hypergeometric functions [38]:

$$f_{\mathrm{e}}(X_k) = \exp\left(-\frac{\xi_k^2X_k^2}{2}\right){}_1F_1\left[\frac{1}{4}(1-\frac{2}{\hbar\omega_k}\epsilon_k); \frac{1}{2}; \xi_k^2X_k^2\right], \tag{a10a}$$

$$f_{\mathrm{o}}(X_k) = \xi_k r_k \exp\left(-\frac{\xi_k^2X_k^2}{2}\right){}_1F_1\left[\frac{1}{4}(3-\frac{2}{\hbar\omega_k}\epsilon_k); \frac{3}{2}; \xi_k^2X_k^2\right], \tag{a10b}$$

with frequencies $\omega_k = 2\sqrt{\kappa/m}\,|\sin(k\pi/N)|$ and $\xi_k = \sqrt{m\omega_k/\hbar}$. Here, the subindices e and o represent the even and odd parities, respectively. In contrast to the eigenenergy of the regular harmonic oscillator, the eigenenergy of the periodic harmonic oscillator ϵ_k is no longer an integer multiple of the frequencies $\hbar\omega_k$. Consequently, the wavefunction of the k-th relative modes within the coordinate range $X_k/LM_1^k \in [-1/2, 1/2]$ is assumed to be

$$\chi_k(X_k) = Af_{\mathrm{e}}(X_k) + Bf_{\mathrm{o}}(X_k) \tag{a11}$$

with undetermined coefficients A and B. Thus, in the next period $X_k/LM_1^k \in [1/2, 3/2]$, according to eq. (a9) the wavefunction can be written as:

$$\chi_k(X_k + LM_1^k) = \mathrm{e}^{\mathrm{i}q_kLM_1^k}\left[Af_{\mathrm{e}}(X_k) + Bf_{\mathrm{o}}(X_k)\right]. \tag{a12}$$

The continuous conditions require both the wavefunction and the derivative of the wavefunction to be continuous, as shown in eq. (27). Since the coefficients A and B cannot be zero simultaneously, the determinant of the coefficient matrix of $\{A, B\}$ should be zero:

$$\begin{vmatrix} f_{\mathrm{e}}(-\frac{l}{2}) - \mathrm{e}^{\mathrm{i}\theta_k}f_{\mathrm{e}}(\frac{l}{2}) & f_{\mathrm{o}}(-\frac{l}{2}) - \mathrm{e}^{\mathrm{i}\theta_k}f_{\mathrm{o}}(\frac{l}{2}) \\ f'_{\mathrm{e}}(-\frac{l}{2}) - \mathrm{e}^{\mathrm{i}\theta_k}f'_{\mathrm{e}}(\frac{l}{2}) & f'_{\mathrm{o}}(-\frac{l}{2}) - \mathrm{e}^{\mathrm{i}\theta_k}f'_{\mathrm{o}}(\frac{l}{2}) \end{vmatrix} = 0 \tag{a13}$$

with $l = LM_1^k$, $\theta_k = q_k l$, and $f'(a) \equiv \frac{\mathrm{d}}{\mathrm{d}X} f(X)\big|_{X=a}$. Finally, we can obtain the constraint for the energy ϵ_k as:

$$f_{\mathrm{o}}\left(\frac{l}{2}\right) f'_{\mathrm{e}}\left(\frac{l}{2}\right) \cos^2\frac{\theta_k}{2} + f_{\mathrm{e}}\left(\frac{l}{2}\right) f'_{\mathrm{o}}\left(\frac{l}{2}\right) \sin^2\frac{\theta_k}{2} = 0, \tag{a14}$$

where we have used the parity of the functions $f_{\mathrm{e}}(X)$ and $f_{\mathrm{o}}(X)$ to simplify eq. (a13). Whether the energy spectrum depends on the total momentum or not depends on $\theta_k \neq 0$. Obviously, for those relative motions with $k > N/2$, their energy spectrum is independent of the total momentum, and thus have no contribution to the decoherence process.

The energy spectrum $\epsilon_k = (n_k + 1/2)\hbar\omega_k$ depends on both the phase factor θ_k and the dimensionless parameter $\xi_k l$, which is shown in Figure a1. In Figure a1(a), the dimensionless parameter is chosen to be $\xi_k l = 5$ and the particle number is $N = 100$. The energy spectrum definitely depends on the phase factor $\theta_k = q_k l$. For those relative motions with $q_k = 0$, the energy spectrum is only determined by the dimensionless parameter, which is in turn determined by the geometry of the ring container and the spring constant. However, for those relative motions with $q_k = \frac{\sqrt{2}n}{\sqrt{N}R}$, the energy spectrum not only depends on the total momentum now, but also forms a group of thin spectra when the total momentum chooses its possible values. In Figure a1(b), the phase factor is chosen as $\theta_k = \pi/2$ and the particle number is $N = 100$. By confining the particles to a smaller ring container via decreasing $\xi_k l$, the energy spectrum deviates greatly from the energy spectrum of a standard harmonic oscillator. When $\xi_k l \gg 1$, the energy spectrum almost coincides with the standard one, which means the effect of the phase factor is also suppressed for a larger ring container or weaker spring constant.

We rewrite eq. (a14) as:

$$\tan^2\frac{\theta_k}{2} = -F(l, \epsilon_k) \tag{a15}$$

with

$$F(l, n_k) = \frac{f_{\mathrm{o}}(\frac{l}{2}) f'_{\mathrm{e}}(\frac{l}{2})}{f_{\mathrm{e}}(\frac{l}{2}) f'_{\mathrm{o}}(\frac{l}{2})}. \tag{a16}$$

To obtain the approximate energy spectrum, which depends linearly on the total momentum, we expand eq. (a15) in the vicinity of the phase factor $\theta_k = \left(\frac{1}{2} + \mu\right)\pi$ and $\xi_k l \gtrsim 1$. In this sense, the approximate energy spectrum is obtained as:

$$\epsilon_k(n, \alpha) = \left(\frac{1}{2} + \alpha' + \delta_k(n, \alpha)\right)\hbar\omega_k, \tag{a17}$$

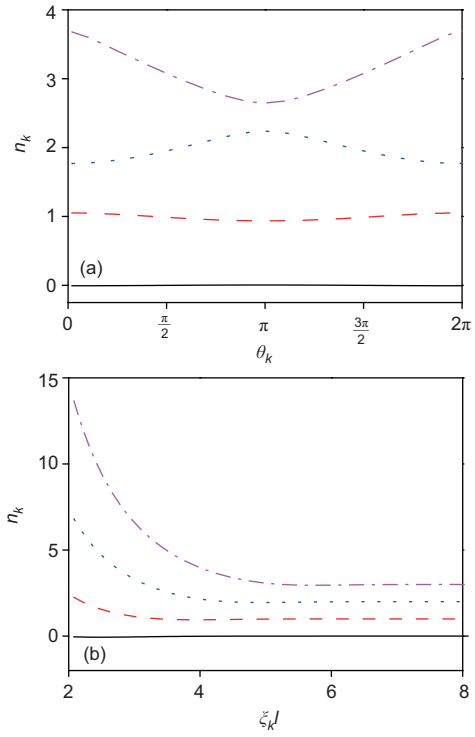

Figure a1 (Color online) (a) Energy spectrum n_k versus phase factor θ_k. The parameters are chosen to be $N = 100$, $\xi_k l = 5$; (b) energy spectrum n_k versus the periodicity $\xi_k l$. The parameters are chosen to be $N = 100$, $\theta_k = \pi/2$. The black dot-dashed line, blue dotted line, red dashed line, and magenta solid line represent the first four eigenstates of the periodic harmonic oscillator. The energy spectrum definitely varies with θ_k, implying the dependence of the total momentum. Moreover, the periodic harmonic oscillator becomes a normal one when $\xi_k l \gg 1$, regardless of θ_k.

where α' is the solution of $F(l, \alpha') = -1$, $\alpha = 0, 1, \ldots$ is a non-negative integer number and the deviation

$$\delta_k(n, \alpha) = g_0(\alpha) + g_1(k, \alpha)\, n \tag{a18}$$

with coefficients

$$g_0(\alpha) = -\frac{1 + F(l, \alpha) + (-1)^{\mu}(1 + 2\mu)\pi}{G(l, \alpha)}, \tag{a19a}$$

$$g_1(k, \alpha) = (-1)^{\mu} 2\pi \frac{M_1^k}{G(l, \alpha)} \frac{\sqrt{2}}{\sqrt{N}}, \tag{a19b}$$

and function $G(l, \alpha) \equiv \frac{\mathrm{d}}{\mathrm{d}n_k} F(l, n_k)\big|_{n_k = \alpha'}$ is the derivative of the function $F(l, n_k)$.